Mineralogy and Petrology (2000) 69: 11–33

Mineralogy and Petrology

Pressure-temperature estimation in orthopyroxene-garnet bearing granulite facies rocks, Bamble Sector, Norway

D. E. Harlov

GeoForschungsZentrum Potsdam, Potsdam, Federal Republic of Germany

With 5 Figures

Received December 2, 1998;
revised version accepted July 10, 1999

Summary

Pressures and temperatures are estimated for the high grade portion (Region D) of the Bamble granulite facies terrane using barometers based on the assemblages almandine-grossular-ferrosilite-anorthite-quartz and pyrope-grossular-enstatite-anorthite-quartz and a garnet-orthopyroxene Fe^{2+}-Mg K_D exchange thermometer based on the experimental data of *Lee* and *Ganguly* (1988). Both barometers utilize the same thermochemical data base (*Berman*, 1988, 1990) and the same garnet (*Berman*, 1990) and orthopyroxene mixing models (*Wood* and *Banno*, 1973; *Sack* and *Ghiorso*, 1989) which are internally consistent both with each other and the *Berman* (1988, 1990) data base. Thus any disagreement between the two barometers is dependent only on the mixing models chosen. When Fe^{2+}-Mg mixing in orthopyroxene and garnet is taken to be ideal, pressures from the two barometers are found to be in poor agreement with $P_{Alm\text{-}Fs}$ ($P_{avg} = 9.2+/-1.0$ kb (1σ)) consistently greater than $P_{Pyr\text{-}En}$ ($P_{avg} = 7.5+/-1.2$ kb (1σ)) by 1.4 to 2.4 kb per sample. If the non-ideal orthopyroxene mixing model of *Sack* and *Ghiorso* (1989) is used and their internally consistent value for mixing on the Fe^{2+}-Mg join in garnet is incorporated in the *Berman* (1990) garnet mixing model, $P_{Alm\text{-}Fs}$ and $P_{Pyr\text{-}En}$ are now in good agreement with the mean pressures for $P_{Alm\text{-}Fs}$ and $P_{Pyr\text{-}En}$ at $7.1+/-0.9$ kb (1σ) and $7.0+/-1.1$ kb (1σ) respectively. Individual pressures per sample are generally within $+/-1$ kb of each other which is within the error range of either barometer. The mean temperature is found to be $793+/-58$ °C (1σ) which is in good agreement with a mean temperature of 795 °C obtained from titaniferous magnetite-ilmenite thermometry (*Harlov*, 1992) as well as the stability fields of sillimanite and Mg-rich cordierite.

Zusammenfassung

Druck-Temperatur-Bestimmung in Orthopyroxen-Granat-führenden granulit-faziellen Gesteinen des Bamble-Sektors, Norwegen

Auf der Grundlage der Paragenesen Almandin-Grossular-Ferrosilit-Anorthit-Quarz und Pyrop-Grossular-Enstatit-Anorthit-Quarz und des auf den experimentellen Daten von *Lee* und *Ganguly* (1988) basierenden Granat-Orthopyroxen-Thermometers (K_D Fe^{2+}-Mg) wurden Drücke und Temperaturen für den hochmetamorphen Anteil (Region D) des granulitfaziellen Terrains von Bamble geschätzt. Beide Barometer stützen sich auf denselben thermochemischen Datensatz (*Berman*, 1988, 1990) und dieselben Mischungsmodelle für Granat (*Berman*, 1990) und Orthopyroxen (*Wood* und *Banno*, 1973; *Sack* und *Ghiorso*, 1989), welche sowohl miteinander als auch mit dem Datensatz von *Berman* (1988, 1990) intern konsistent sind. Somit hängt jegliche Abweichung zwischen den beiden Barometern nur vom gewählten Mischungsmodell ab. Bei Annahme idealer Mischung von Fe^{2+} und Mg im Orthopyroxen ist die Übereinstimmung der mit den beiden Barometern berechneten Drücke schlecht, wobei $P_{Alm\text{-}Fs}$ ($P_{avg} = 9{,}2 \pm 1{,}0$ kbar (1σ)) für die einzelnen Proben durchweg um 1,4 bis 2,4 kbar größer ist als $P_{Pyr\text{-}En}$ ($P_{avg} = 7{,}5 \pm 1{,}2$ kbar (1σ)). Bei Anwendung des nichtidealen Mischungsmodells für Orthopyroxen von *Sack* und *Ghiorso* (1989) und bei Integration ihres intern konsistenten Mischungsparameters für die Reihe Fe^{2+}-Mg-Granat in das Mischungsmodell für Granat von *Berman* (1990) sind $P_{Alm\text{-}Fs}$ und $P_{Pyr\text{-}En}$ in guter Übereinstimmung mit den Durchschnittsdrücken für $P_{Alm\text{-}Fs}$ und $P_{Pyr\text{-}En}$ ($7{,}1 \pm 0{,}9$ kbar (1σ) bzw. $7{,}0 \pm 1{,}1$ kbar (1σ)). Die für die einzelnen Proben erhalten Drücke variieren im allgemeinen nur um ± 1 kbar, d.h. im Fehlerbereich beider Barometer. Für die Durchschnittstemperatur wurden 793 ± 58 °C (1σ) ermittelt. Diese ist sowohl mit der durch Ti-Magnetit/Ilmenit-Thermometrie (*Harlov*, 1992) bestimmten mittleren Temperatur von 795 °C als auch mit den Stabilitätsfeldern von Sillimanit und Mg-reichem Cordierit in guter Übereinstimmung.

Introduction

Estimation of pressures and temperatures in a number of orthopyroxene-garnet bearing granulite facies terranes over the last 15 years has incorporated two widely used barometers, almandine-grossular-ferrosilite-anorthite-quartz and pyrope-grossular-enstatite-anorthite-quartz, which in turn have utilized a wide array of garnet mixing models while assuming that Fe^{2+}-Mg mixing in orthopyroxene is nearly ideal (e.g. *Bohlen* et al., 1983; *Newton* and *Perkins*, 1982; *Perkins* and *Chipera*, 1985) or else have not taken into account ordering between the M1 and M2 sites in orthopyroxene (cf. *Berman* and *Aranovich*, 1996). Often though, the question of internal consistency between these two barometers and the thermochemical data bases and mixing models that they utilize is not brought into question.

Lal (1993) has correlated both barometers and an Fe^{2+}-Mg garnet-orthopyroxene exchange thermometer as an internally consistent recalibration based principally on the reversed data of *Bohlen* et al. (1980, 1983) and a variety of Fe^{2+}-Mg exchange data between garnet and orthopyroxene including *Lee* and *Ganguly* (1988). Internal consistency is guaranteed by deriving the enstatite-pyrope-grossular-anorthite-quartz barometer directly from the difference between the equilibrium for the ferrosilite-almandine-grossular-anorthite-quartz barometer and the equilibrium for the garnet-orthopyroxene Fe^{2+}-Mg exchange thermometer –

both of which *Lal* (1993) directly calibrates from the experimental data of *Bohlen* et al. (1980, 1983) and *Lee* and *Ganguly* (1988). As a consequence there is nearly perfect agreement between the two barometers for a unique temperature. Fe^{2+}-Mg mixing in garnet and orthopyroxene is made internally consistent via the experimentally calibrated Fe^{2+}-Mg orthopyroxene-garnet exchange data of *Lee* and *Ganguly* (1988) after certain assumptions concerning Fe^{2+}-Mg mixing in garnet are made – namely that it is relatively close to ideality. The remaining Margules parameters are taken, after due consideration, from a variety of sources. While such an internally consistent compilation certainly has its uses for the working field petrologist, especially since the approximate pressures and temperatures of 8 kbars and 800 °C are obtained the majority of the time for the majority of granulite facies terranes, it has no relevance with respect to evaluating either independently determined internally consistent mineral endmember thermochemical data bases or independently calibrated solid solution mixing models for either garnet or orthopyroxene which are themselves internally consistent with these data bases.

The goal of this present study is to explore the ramifications of assuming either ideal or non-ideal Fe^{2+}-Mg mixing in orthopyroxene and garnet as applied to the almandine-grossular-ferrosilite-anorthite-quartz and pyrope-grossular-enstatite-anorthite-quartz barometers in conjunction with the experimentally calibrated garnet-orthopyroxene Fe^{2+}-Mg K_D exchange thermometer of *Lee* and *Ganguly* (1988), the thermochemical endmember mineral database of *Berman* (1988, 1990) and both ideal and non ideal Fe^{2+}-Mg mixing models for garnet and orthopyroxene which are internally consistent with *Berman* (1988, 1990) for 36 garnet-orthopyroxene-plagioclase-quartz bearing samples from the highest grade portion of the Bamble granulite facies terrane, S.E. Norway and to compare the results of these pressure-temperature estimations with independent estimations from other mineral assemblages.

Regional geology

The Bamble Sector extends for a 100 km along the southeastern coast (Skaggerak) of Norway (Fig. 1) reaching a maximum width of 25 km (*Starmer*, 1985, 1986). It consists of Middle Proterozoic supracrustals intruded, deformed and metamorphosed during the Gothian [Kongsbergian] orogeny (1.540 Ga) (*Field* et al., 1985) which later underwent high grade metamorphism during the Sveconorwegian [Grenvillian] orogeny (1150–1070 Ga) (*Kullerud* and *Dahlgren*, 1993; *Hagelia*, 1995). The Bamble Sector increases in metamorphic grade from the northwest to the southeast culminating in a 5–10 km wide strip of granulite facies gneiss which extends 40 km northeastward from the town of Arendal along the Skaggerak coast. Sillimanite is the stable aluminosilicate throughout the Bamble Sector though retrograde kyanite is found in amphibolite facies north of Tvedestrand (*Touret* and *Falkum*, 1984).

Variations in mineralogy and geochemistry have been used to divide the Bamble Sector up into four regions labeled A–D which run roughly parallel to the coast (Fig. 1) (*Field* et al., 1980; *Smalley* et al., 1983; *Lamb* et al., 1986). Region A (amphibolite facies) and Region B (granulite facies) consist primarily of acid to

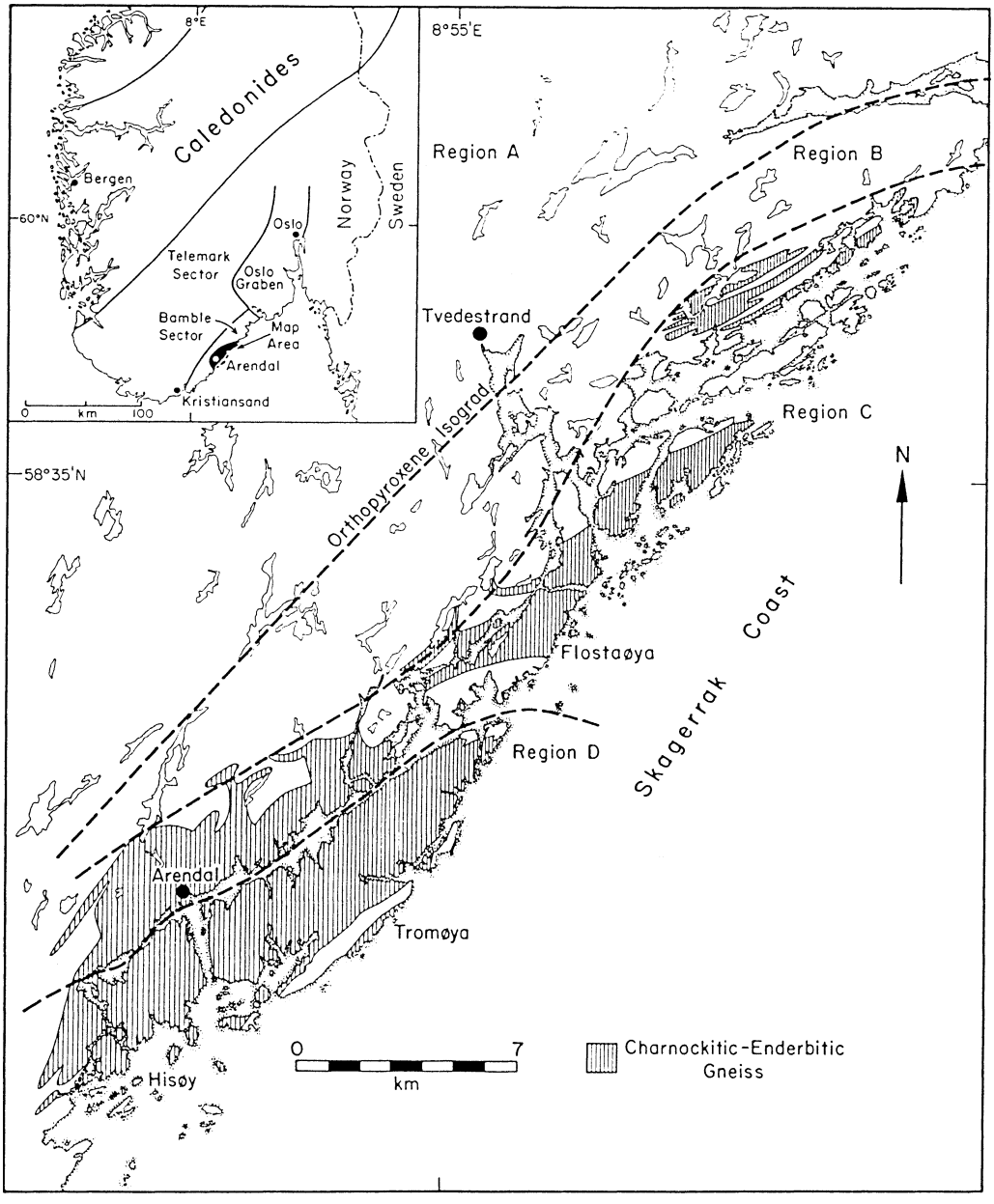

Fig. 1. The Bamble Sector, S.E. Norway showing the location of regions A through D as well as the location of the orthopyroxene isograd. Regional distribution of granulites in Region C (charnockites) and Region D (enderbites) is taken from *Starmer* (1985, 1986)

intermediate host gneisses with a broadly granitic mineralogy separated by an orthopyroxene isograd in the metabasite intrusives. Region C marks the first occurrence of charnockitic gneiss (K-feldspar-plagioclase-orthopyroxene-quartz). Region D, the highest grade portion of the Bamble Sector and the source for most of the samples used in this study, makes up the islands of Tromøya and Hisøya. This region contains a dark green, well jointed, poorly foliated, tonalitic-

Table 1. *Mineralogy of samples*

Sample	Qtz	Plg	Kfs	Opx	Cpx	Gt	Am	Bt	Ch	Ap	Zi	Mt	Ilm	Hm	Py	Cl	Other
86-BD-17	X	X	X	X		X		X		X	X	X	lmX	lm	X	X	Mo
86-BD-26	X	X		X		X		X		X	X	X	lmX	lm	X	X	
86-BD-50	X	X		X		X				X	X	X	lmX	lm	X	X	Mo
86-BD-58	X	X		X		X	X	X		X	X	X	lmX		X	X	
86-BD-59	X	X		X		X	X	X	X	X	X	X	lmX		X	X	
86-BD-60	X	X		X		X	X		X	X	X	X	lmX	lm	X	X	
86-BD-68	X	X		X		X				X	X	X	lm		X	X	
86-BD-73	X	X		X		X		X		X	X	X	lmX	lm	X	X	Mo
86-BD-74	X	X		X		X		X	X	X	X	X	lmX	lm	X	X	
86-BD-79	X	X		X		X		X	X	X	X	X	X				Mu
86-BD-81	X	X		X	X	X	X			X	X	X	lmX	lm			
86-BD-83	X	X		X		X	X			X	X	X	lmX	lm			
86-BD-95	X	X		X		X		X	X	X	X	X	lmX		X	X	
86-BD-102	X	X		X		X		X		X	X	X	lmX		X	X	
86-BD-136	X	X		X		X	X	X		X	X	X	X	lm	X	X	
86-BD-140	X	X		X		X		X		X	X	X	lmX	lm	X		
86-BD-141	X	X		X		X		X		X	X	X	X	lm	X	X	Mo
86-BD-142	X	X		X		X		X		X	X	X	lm		X	X	
86-BD-143	X	X		X		X	X			X	X	X	lmX	lm		X	
86-BD-301	X	X	X	X		X	X		X	X	X	X	lm			X	
86-BD-305	X	X		X		X				X	X	X	X	lm	X	X	
86-BD-307	X	X		X		X	X	X	X	X	X		X	lm			
86-BD-310	X	X		X		X		X		X	X	X	lmX	lm	X	X	
86-BD-312	X	X		X		X		X	X	X	X	X	lmX		X	X	
86-BD-321	X	X		X		X		X		X	X	X	lmX		X		Mo
86-BD-323	X	X	X	X		X		X		X	X	X	lmX		X	X	
86-BD-324	X	X		X		X		X		X	X	X	lmX	lm	X		
86-BC-174	X	X	X	X		X		X		X	X	X			X	X	
86-BC-276	X	X		X		X		X	X	X	X	X	X		X	X	Mo
86-BC-298	X	X		X		X	X	X		X	X	X	X				Mo, He
86-BC-325	X	X		X		X		X		X	X	X	lmX	lm	X	X	
84-AR-8	X	X		X		X		X		X	X	X	lmX	lm			Mo, Mu
84-AR-10	X	X		X		X		X	X	X	X	X	lmX	lm	X		Mu
84-AR-11	X	X		X	X	X		X		X	X	X	lmX	lm			Cd, Ru
84-AR-19	X	X		X		X	X		X	X	X	X	lmX		X	X	
84-TV-6	X	X		X		X	X	X	X	X	X	X			X		

Am Amphibole, *Ap* Apatite, *Bt* Biotite, *Cl* Chalcopyrite, *Ch* Chlorite, *Cd* Cordierite, *Cpx* Clinopyroxene, *Gt* Garnet, *He* Hercynite, *Hm* Hematite, *Ilm* Ilmenite, *Kfs* K-feldspar, *Mt* Magnetite, *Mo* Monazite, *Mu* Muscovite, *Opx* Orthopyroxene, *Pl* Plagioclase, *Py* Pyrrhotite, *Qtz* Quartz, *Ru* Rutile, *Zi* Zircon, *lm* lamellae (for Ilmenite these lamellae are in the Titaniferous Magnetite grains, for Hematite these lamellae are in the Ilmenite grains)

trondhjemitic ''enderbitic'' gneiss (plagioclase-orthopyroxene-quartz) which is characterized, along with the metabasite intrusions, by extremely low concentrations of K-feldspar, rare earth elements (REE), large ion lithophiles (LIL), especially Rb (*Field* et al., 1985; *Lamb* et al., 1986), as well as low concentrations of chalcophile elements, especially Au, Sb, As, and S (*Cameron* et al., 1993). A late brittle normal fault, located beneath the Tromoysund, separates Region D from C (*Starmer*, 1985, 1986). The mineralogy of the samples used in this study are summed up in Table 1.

The gneisses of Regions C and D are also characterized by abundant high density CO_2 fluid inclusions and high density brine inclusions (*Touret*, 1985). These fluid inclusions have been suggested to represent evidence for pervasive flow of high grade, low H_2O activity fluids through these rocks which essentially dehydrated what were initially amphibolite grade rocks to charnockites and enderbites during granulite facies metamorphism (cf. *Touret*, 1985; *Visser* and *Senior*, 1990; *Harlov*, 1992; *Harlov* et al., 1998).

Analytical method

Major and minor elements were obtained at the University of Wisconsin using an ARL-SEMQ electron microprobe with nine wavelength despersive crystal spectrometers (PET, LIF and TAP). An accelerating potential of 15 kV and an emission current of 100 μA were employed. Sample current ranged from 20 to 40 nA. In order to identify major and minor elements present ($Z > 11$) at a level above 0.01 weight percent, emission spectra were obtained using an energy dispersive Li-silicon detector over a 500 second counting period. The beam current was digitized for quantitative analysis with counting times of 40 seconds for each spot. Measurement of temperatures and pressures nearest to peak metamorphic conditions for these rocks was ensured by only analyzing the interior region of the garnet, orthopyroxene, and plagioclase grains while the area within 100–200 microns of the grain edge was scrupulously avoided. Analysis consisted of taking 5 to 20 spots uniformly distributed over the surface of the grain interior and then averaging these analyses together per grain. None of these grain interiors were found to be zoned. However garnet grain rims showed some enrichment in Fe that was 2–3 percent higher than the amount of Fe in the grain interior. This increase in Fe is most likely due to partial re-equilibration during cooling and uplift after peak metamorphism. Orthopyroxene grain rims, when sampled, showed no such enrichment in Fe nor any enrichment in Al. In the analysis of plagioclase and cordierite a broad 30 μm beam was used. Standardization was repeated after every 5 to 6 grain analyses in order to check for drift. Natural garnet, orthopyroxene, clinopyroxene, rhodonite, fayalite, albite, microcline and anorthite were used as standards. Microprobe data for garnet, orthopyroxene, clinopyroxene, plagioclase and cordierite were reduced to oxide weight percents using the technique outlined in *Bence* and *Albee* (1968). The amount of Fe^{3+} in garnet or orthopyroxene was determined via charge balancing and stoichiometry. Error for the major elements is estimated to be within $+/-3$ percent of the amount present. Up to five grains of each mineral were analyzed per sample and then, because of the uniform composition of the grain interiors, averaged to give the composite garnet, pyroxene, and plagioclase oxide weight percent analyses in Table 2 and the element fractions in Table 3. All pressure and temperature estimations were made using these composite analyses.

Thermodynamic considerations

Thermometry

Temperatures were obtained using the experimentally calibrated garnet-orthopyroxene Fe^{2+}-Mg K_D exchange thermometer of *Lee* and *Ganguly* (1988) which is

Table 2. *Garnet analyses*

	BD-17	BD-26	BD-50	BD-58	BD-59	BD-60	BD-68	BD-73	BD-74
# grains	5	1	2	3	3	4	3	3	3
SiO_2	37.51	37.89	37.62	37.34	37.55	37.02	38.13	38.66	37.59
Al_2O_3	21.90	21.32	21.39	20.97	21.16	21.08	21.39	21.54	21.93
Fe_2O_3	0.33	0.05	0.32	0.18	1.04	1.96	0.00	0.15	1.22
FeO	26.63	28.30	28.49	29.07	28.98	27.56	31.59	29.17	27.78
MnO	6.43	4.40	2.91	2.32	1.76	2.13	1.35	1.21	1.11
MgO	5.77	6.57	4.52	3.19	3.52	3.55	6.05	7.83	7.85
CaO	1.04	0.66	4.28	5.74	6.13	6.43	1.06	1.24	1.60
Total	99.61	99.19	99.53	98.81	100.14	99.73	99.57	99.80	99.08

	BD-79	BD-81	BD-83	BD-95	BD-102	BD-136	BD-140	BD-141	BD-142
# grains	2	6	5	3	2	2	5	3	2
SiO_2	38.24	37.06	38.22	37.23	37.73	38.22	38.74	38.45	38.52
Al_2O_3	22.36	21.04	20.52	21.46	22.36	22.62	21.19	22.15	22.43
Fe_2O_3	0.98	1.56	1.17	1.28	0.26	1.33	0.80	0.13	0.45
FeO	28.89	28.47	28.83	26.40	30.63	27.13	29.89	30.25	24.52
MnO	1.33	1.97	1.93	4.84	4.04	1.06	1.73	0.98	2.80
MgO	8.05	2.78	3.58	4.69	4.93	6.22	7.45	7.61	9.76
CaO	0.93	6.94	6.59	3.79	1.23	5.01	1.10	0.85	1.03
Total	100.78	99.82	100.84	99.69	101.18	101.59	100.90	100.42	99.51

	BD-143	BD-301	BD-305	BD-307	BD-310	BD-312	BD-321	BD-323	BD-324
# grains	2	2	2	2	2	3	2	2	2
SiO_2	38.27	36.91	37.76	37.84	37.73	37.28	38.70	38.79	37.79
Al_2O_3	21.76	20.06	22.13	22.32	21.27	21.16	20.07	21.94	22.21
Fe_2O_3	0.03	0.95	2.68	2.25	0.32	0.03	1.31	0.18	1.22
FeO	26.68	29.27	24.73	27.06	28.37	31.52	29.45	28.96	28.10
MnO	3.21	2.65	1.78	1.18	4.96	2.54	1.18	1.57	3.49
MgO	5.27	1.82	10.03	9.19	5.35	3.16	8.14	8.27	6.91
CaO	4.99	6.99	0.58	0.49	1.65	3.36	0.88	0.86	0.97
Total	100.21	98.65	99.69	100.33	99.65	99.05	99.73	100.57	100.69

	AR-8	AR-10	AR-11	AR-19	BC-174	BC-276	BC-298	BC-325	TV-6
# grains	2	3	3	3	2	2	2	3	1
SiO_2	37.32	37.43	39.16	38.20	37.33	37.35	38.93	38.03	37.49
Al_2O_3	21.87	22.22	22.52	21.11	21.23	20.38	22.36	21.75	21.26
Fe_2O_3	0.00	0.00	0.00	0.00	0.67	1.61	0.09	1.20	1.66
FeO	28.74	29.68	26.15	28.82	30.21	23.44	28.37	30.27	27.29
MnO	4.19	1.58	0.41	2.10	1.26	7.16	1.52	2.11	1.54
MgO	6.11	7.20	11.15	2.88	3.41	3.40	9.11	6.01	4.73
CaO	0.47	0.45	0.23	6.43	5.53	6.18	0.32	1.83	5.89
Total	98.70	98.56	99.62	99.54	99.64	99.52	100.70	101.20	99.86

(continued)

Table 2 (continued). *Pyroxene analyses*

	BD-17	BD-26	BD-50	BD-58	BD-59	BD-60	BD-68	BD-73	BD-74
# grains	3	1	2	3	3	3	3	2	3
SiO_2	49.94	50.00	49.51	49.53	49.19	49.34	49.43	49.71	49.81
Al_2O_3	2.06	2.05	1.66	1.18	1.17	1.20	2.67	3.58	3.31
Fe_2O_3	1.07	1.60	0.97	0.17	0.62	1.50	0.53	0.83	0.89
FeO	25.92	24.81	28.49	32.91	32.86	31.64	29.10	25.20	25.75
MnO	2.03	1.34	1.00	0.86	0.70	0.89	0.42	0.40	0.35
MgO	17.66	18.81	16.35	13.81	13.66	14.30	16.46	18.85	18.61
CaO	0.21	0.08	0.45	0.63	0.71	0.76	0.19	0.20	0.22
Total	98.89	98.69	98.43	99.09	98.91	99.63	98.80	98.77	98.94

	BD-79	BD-81	BD-83	BD-95	BD-102	BD-136	BD-140	BD-141	BD-142
# grains	3	4	3	3	2	2	3	2	2
SiO_2	49.37	48.96	49.52	49.78	48.80	49.56	49.35	49.27	49.54
Al_2O_3	4.55	0.91	1.03	1.46	1.99	2.29	3.56	4.34	5.32
Fe_2O_3	1.96	1.34	0.33	1.00	1.45	1.94	0.38	1.34	2.87
FeO	24.46	34.36	32.30	28.77	29.40	26.31	27.35	26.83	19.07
MnO	0.36	0.86	0.76	1.98	1.25	0.38	0.54	0.30	0.79
MgO	19.08	12.47	14.17	15.79	15.39	17.95	17.27	17.72	21.97
CaO	0.16	0.85	0.70	0.48	0.21	0.46	0.12	0.17	0.17
Total	99.94	99.75	98.81	99.26	98.49	98.89	98.57	99.97	99.73

	BD-143	BD-301	BD-305	BD-307	BD-310	BD-312	BD-321	BD-323	BD-324
# grains	2	2	2	1	2	3	2	2	2
SiO_2	50.55	47.81	49.23	49.50	48.58	48.91	49.67	48.91	49.14
Al_2O_3	1.78	0.70	5.53	4.91	1.93	1.28	3.18	4.61	3.36
Fe_2O_3	1.99	0.47	1.93	0.01	3.28	0.68	1.69	1.68	1.67
FeO	25.93	39.04	21.74	25.22	26.56	33.82	25.93	24.55	25.03
MnO	1.13	1.31	0.55	0.32	1.59	0.91	0.33	0.44	1.07
MgO	18.34	8.75	20.42	18.77	16.60	12.98	18.45	18.67	18.20
CaO	0.54	0.94	0.14	0.15	0.26	0.47	0.20	0.18	0.17
Total	100.26	99.02	99.54	98.88	98.80	99.05	99.45	99.04	98.64

	AR-8	AR-10	AR-11	AR-19	BC-174	BC-276	BC-298	BC-325	TV-6
# grains	3	2	4	3	2	2	2	3	1
SiO_2	49.86	47.84	49.48	49.90	48.86	49.43	48.71	49.57	49.82
Al_2O_3	3.56	4.58	6.55	0.97	1.20	0.83	5.28	2.55	0.90
Fe_2O_3	0.00	4.00	0.30	0.14	0.87	1.08	1.74	0.58	1.87
FeO	26.51	23.15	20.53	32.60	33.22	28.05	23.22	28.92	29.16
MnO	1.08	0.44	0.12	0.77	0.54	3.20	0.48	0.71	0.64
MgO	17.64	18.75	21.57	13.64	13.34	15.03	19.30	16.44	16.12
CaO	0.08	0.15	0.03	0.62	0.70	0.81	0.12	0.26	0.81
Total	98.73	98.91	98.58	98.64	98.73	98.43	98.85	99.03	99.32

(continued)

Table 2 (continued). *Plagioclase analyses*

	BD-17	BD-26	BD-50	BD-58	BD-59	BD-60	BD-68	BD-73	BD-74
# grains	3	2	2	3	3	3	2	3	3
SiO_2	65.92	65.51	59.85	58.29	58.23	57.47	65.88	63.46	61.74
Al_2O_3	21.40	20.89	26.71	26.33	26.33	27.05	21.53	23.62	23.75
CaO	1.86	1.99	7.51	7.73	8.21	8.69	2.78	3.91	5.00
Na_2O	10.26	10.38	7.18	6.86	6.71	6.36	10.30	9.16	8.59
K_2O	0.42	0.31	0.45	0.48	0.42	0.49	0.33	0.37	0.31
Total	99.86	99.08	101.70	99.69	99.90	100.06	100.82	100.52	99.39

	BD-79	BD-81	BD-83	BD-95	BD-102	BD-136	BD-140	BD-141	BD-142
# grains	2	2	3	3	2	2	4	3	2
SiO_2	62.56	59.68	57.99	61.02	65.20	54.98	64.89	65.03	63.04
Al_2O_3	22.56	26.27	26.30	23.57	21.20	27.49	21.63	22.01	23.32
CaO	3.14	7.52	8.51	5.53	2.55	10.07	2.98	2.75	3.91
Na_2O	9.87	7.00	6.43	8.09	9.74	5.87	9.27	9.92	8.82
K_2O	0.20	0.39	0.28	0.54	0.81	0.29	0.65	0.28	0.28
Total	98.33	100.86	99.51	98.75	99.50	98.70	99.42	99.99	99.37

	BD-143	BD-301	BD-305	BD-307	BD-310	BD-312	BD-321	BD-323	BD-324
# grains	2	2	2	2	2	3	2	1	2
SiO_2	58.36	61.10	65.83	66.42	63.88	62.13	64.25	64.76	64.22
Al_2O_3	26.42	25.71	21.59	21.45	21.93	23.89	22.76	21.73	22.81
CaO	7.89	6.13	2.28	1.89	3.15	5.08	2.84	2.10	3.31
Na_2O	6.87	8.02	9.91	10.17	9.62	8.62	10.10	9.99	9.60
K_2O	0.21	0.40	0.58	0.54	0.85	0.44	0.39	0.24	0.45
Total	99.75	101.36	100.19	100.47	99.43	100.16	100.34	98.82	100.39

	AR-8	AR-10	AR-11	AR-19	BC-174	BC-276	BC-298	BC-325	TV-6
# grains	2	4	2	3	2	3	2	3	2
SiO_2	65.87	65.51	65.64	57.76	60.13	61.15	67.13	66.05	55.82
Al_2O_3	21.00	21.09	20.81	26.93	26.51	24.58	20.67	21.75	28.18
CaO	1.54	1.50	1.32	8.60	7.53	5.64	0.98	3.90	9.69
Na_2O	10.44	10.46	10.68	6.37	6.62	8.13	10.33	8.84	5.80
K_2O	0.82	0.56	0.39	0.39	0.66	0.62	0.35	0.70	0.31
Total	99.67	99.22	98.84	100.05	101.45	100.12	99.64	101.24	99.80

based on the equilibrium:

$$\underset{\text{Pyrope}}{1/3Mg_3Al_2Si_3O_{12}} + \underset{\text{Ferrosilite}}{FeSiO_3} = \underset{\text{Almandine}}{1/3Fe_3Al_2Si_3O_{12}} + \underset{\text{Enstatite}}{MgSiO_3} \quad (1)$$

While the partitioning of Fe^{2+} and Mg between garnet and orthopyroxene is less pronounced than for most other Fe^{2+}-Mg K_D exchange thermometers involving

Table 3. *Garnet, orthopyroxene, and plagioclase molar fractions*

	Garnet				Orthopyroxene				Plagioclase		
Sample	X_{Alm}	X_{Pyr}	X_{Gr}	X_{Sp}	X_{Fs}	X_{En}	X_{Wol}	X_{Pm}	X_{An}	X_{Ab}	X_{Or}
BD-17	0.595	0.230	0.030	0.145	0.420	0.511	0.004	0.033	0.089	0.887	0.024
BD-26	0.625	0.258	0.019	0.098	0.400	0.541	0.002	0.022	0.094	0.889	0.017
BD-50	0.633	0.179	0.122	0.066	0.469	0.479	0.009	0.017	0.357	0.618	0.025
BD-58	0.654	0.128	0.165	0.053	0.547	0.409	0.013	0.014	0.373	0.599	0.028
BD-59	0.645	0.140	0.175	0.040	0.548	0.406	0.015	0.012	0.394	0.582	0.024
BD-60	0.622	0.143	0.186	0.049	0.523	0.421	0.016	0.015	0.418	0.554	0.028
BD-68	0.701	0.239	0.030	0.030	0.476	0.479	0.004	0.007	0.127	0.855	0.018
BD-73	0.634	0.304	0.035	0.027	0.404	0.539	0.004	0.006	0.187	0.792	0.021
BD-74	0.618	0.311	0.046	0.025	0.413	0.532	0.004	0.006	0.239	0.744	0.017
BD-79	0.632	0.313	0.026	0.029	0.388	0.539	0.003	0.006	0.148	0.841	0.011
BD-81	0.642	0.112	0.201	0.045	0.575	0.372	0.018	0.015	0.364	0.614	0.022
BD-83	0.632	0.140	0.185	0.043	0.538	0.420	0.015	0.013	0.416	0.568	0.016
BD-95	0.593	0.188	0.109	0.110	0.472	0.461	0.010	0.033	0.265	0.704	0.031
BD-102	0.679	0.195	0.035	0.091	0.487	0.454	0.004	0.021	0.120	0.834	0.046
BD-136	0.594	0.243	0.140	0.023	0.426	0.518	0.009	0.006	0.479	0.505	0.016
BD-140	0.645	0.287	0.030	0.038	0.444	0.500	0.003	0.009	0.145	0.817	0.038
BD-141	0.659	0.295	0.024	0.022	0.429	0.504	0.003	0.005	0.131	0.853	0.016
BD-142	0.532	0.378	0.029	0.061	0.297	0.609	0.003	0.012	0.193	0.790	0.017
BD-143	0.584	0.205	0.140	0.071	0.414	0.522	0.011	0.018	0.383	0.605	0.012
BD-301	0.663	0.073	0.203	0.061	0.675	0.269	0.021	0.023	0.291	0.687	0.022
BD-305	0.548	0.396	0.016	0.040	0.342	0.572	0.003	0.009	0.109	0.858	0.033
BD-307	0.598	0.362	0.014	0.026	0.403	0.534	0.003	0.005	0.090	0.879	0.031
BD-310	0.629	0.212	0.047	0.112	0.436	0.486	0.005	0.026	0.146	0.807	0.047
BD-312	0.716	0.128	0.098	0.058	0.567	0.388	0.010	0.015	0.239	0.736	0.025
BD-321	0.637	0.313	0.024	0.026	0.416	0.527	0.004	0.005	0.132	0.847	0.021
BD-323	0.624	0.318	0.024	0.034	0.393	0.532	0.004	0.007	0.103	0.883	0.014
BD-324	0.621	0.273	0.028	0.078	0.404	0.524	0.004	0.018	0.156	0.819	0.025
AR-8	0.645	0.245	0.014	0.096	0.429	0.508	0.002	0.018	0.072	0.883	0.045
AR-10	0.664	0.287	0.013	0.036	0.372	0.537	0.003	0.007	0.071	0.897	0.032
AR-11	0.560	0.425	0.006	0.009	0.321	0.602	0.001	0.002	0.063	0.915	0.022
AR-19	0.650	0.116	0.186	0.048	0.545	0.406	0.013	0.013	0.417	0.560	0.023
BC-174	0.677	0.136	0.159	0.028	0.557	0.398	0.015	0.009	0.371	0.591	0.038
BC-276	0.525	0.136	0.177	0.162	0.466	0.445	0.017	0.054	0.268	0.697	0.035
BC-298	0.609	0.349	0.009	0.033	0.370	0.548	0.002	0.008	0.049	0.930	0.021
BC-325	0.665	0.236	0.052	0.047	0.472	0.478	0.005	0.012	0.188	0.772	0.040
TV-6	0.609	0.188	0.168	0.035	0.478	0.471	0.017	0.011	0.471	0.511	0.018

Alm Almandine; *Pyr* Pyrope; *Gr* Grossular; *Sp* Spessartine; *Fs* Ferrosilite; *En* Enstatite; *Wol* Wollastonite; *Pm* Pyroxmangite; *An* Anorthite; *Ab* Albite; *Or* Orthoclase

garnet, it is still reasonably large ($K_D = 1.5$–5) at granulite facies pressures and temperatures (*Lee* and *Ganguly*, 1988). Another advantage is that since garnet and orthopyroxene are relatively refractory minerals compared to most other Fe^{2+}-Mg silicates, they have much higher stopping temperatures (*Lee* and *Ganguly*, 1988).

Lee and *Ganguly* (1988) obtained Fe^{2+}-Mg fractionation data (principally as a series of half reversals over $X_{Alm} = 0.2$ to 0.9) between co-existing garnet and orthopyroxene grains (both synthetic and natural) at pressures of 20–45 kb and temperatures of 975–1400 °C using graphite capsules and a PbO/PbF flux to facilitate the reaction. In calibrating an Fe^{2+}-Mg garnet-orthopyroxene K_D exchange thermometer, the linear fit to the $RT\ln K_D$ vs. temperature data of *Lee* and *Ganguly* (1988; their Fig. 4) was used instead of their non-linear fit. The ΔH_f ($-3916+/-282$ cal) for this exchange reaction (Eq. 1) derived from the linear fit at 750 °C agrees very well with the ΔH_f derived from calorimetric enthalpies at the same temperature ($-3921+/-755$) (cf. *Lee* and *Ganguly*, 1988). In contrast the ΔH_f value ($-2607+/-183$ cal) for the non-linear fit, extrapolated to 750 °C, shows poor agreement with the calorimetric value. Volume data, including expansivity's and compressibility's, were taken from *Berman* (1988, 1990). The Margules parameters for ΔW_{Ca} and ΔW_{Mn} were taken from *Berman* (1990). The garnet-orthopyroxene Fe^{2+}-Mg K_D exchange data of *Lee* and *Ganguly* (1988) have recently been re-confirmed in the Fe-rich range in a limited series of garnet-orthopyroxene Fe^{2+}-Mg K_D exchange experiments by *Eckert* and *Bohlen* (1992).

Barometry

Two widely used barometers were applied to the samples. The first barometer (Pyr-En) is based on the equilibrium:

$$\underset{\text{Pyrope}}{2Mg_3Al_2Si_3O_{12}} + \underset{\text{Grossular}}{Ca_3Al_2Si_3O_{12}} + \underset{\text{Quartz}}{3SiO_2} = \underset{\text{Enstatite}}{3Mg_2Si_2O_6} + \underset{\text{Anorthite}}{3CaAl_2Si_2O_8} \quad (2)$$

(cf. *Newton* and *Perkins*, 1982; *Perkins* and *Chipera*, 1985; *Lal*, 1993).

The second barometer (Alm-Fs) is based on the equilibrium:

$$\underset{\text{Almandine}}{2Fe_3Al_2Si_3O_{12}} + \underset{\text{Grossular}}{Ca_3Al_2Si_3O_{12}} + \underset{\text{Quartz}}{3SiO_2} = \underset{\text{Ferrosilite}}{3Fe_2Si_2O_6} + \underset{\text{Anorthite}}{3CaAl_2Si_2O_8} \quad (3)$$

(cf. *Bohlen* et al., 1983; *Perkins* and *Chipera*, 1985; *Harlov*, 1992; *Lal*, 1993).

Pressures from either equilibrium can be evaluated using the following relationship:

$$\Delta G_r(P,T) = \Delta H_r(T) - T(K)\Delta S_r(T) + \int_{P_r}^{P} \left\{ V(P_r,T_r) - T\left(\frac{\partial V}{\partial T}\right)_P + T\left(\frac{\partial V}{\partial P}\right)_T \right\} dP + RT\ln K_{eq} = 0 \quad (4)$$

where ΔG_r, ΔH_r, and ΔS_r are, respectively, stoichiometric changes in the Gibbs free energy, the enthalpy, and the entropy for equilibria (2) and (3) at some pressure

and known temperature (cf. *Berman*, 1988). Inherent in the volume term, V(P,T), are compressibility and expansivity coefficients where:

$$V(P,T) = V(P_r,T_r)(1 + v_1(P - P_r) + v_2(P - P_r)^2 + v_3(T - T_r) + v_4(T - T_r)^2) \tag{5}$$

Here the expansivity (v_3 and v_4) and compressibility coefficients (v_1 and v_2) are taken from *Berman* (1988, 1990). K_{eq}, as the ratio of the activities, allows for a departure from this stoichiometry and is given by:

$$K_{eq} = \frac{\alpha_{An}^3 \alpha_{En}^3}{\alpha_{Gt}^2 \alpha_{Gr}} \tag{6}$$

where $\alpha_{An}, \alpha_{En}, \alpha_{Gr}$, and α_{Gt} are the anorthite, enstatite, grossular and pyrope or almandine activities, respectively.

In this study, all thermochemical endmember parameters are taken from the internally consistent data set of *Berman* (1988, 1990), in part, because the garnet and orthopyroxene mixing models chosen in this study have been calibrated to be internally self consistent with *Berman* (1988, 1990) and not with *Holland* and *Powell* (1990). An overall error range of +/−1 kilobar, based both on the microprobe data and the uncertainty inherent in the thermochemical data base used (*Berman*, 1988, 1990), is adopted for both barometers. This uncertainty agrees with estimates by previous authors (cf. *Newton* and *Perkins*, 1982; *Perkins* and *Chipera*, 1985; *Moecher* et al., 1988).

Mixing models

When calibrating either the Alm-Fs and/or Pyr-En barometers, Fe^{2+}-Mg mixing in orthopyroxene is assumed by most authors, e.g. *Newton* and *Perkins* (1982), *Bohlen* et al. (1983), *Perkins* and *Chipera* (1985), *Berman* (1990), to be close to ideality such that at granulite facies pressures and temperatures, Fe^{2+} and Mg are both equally distributed between, and mix ideally on, the M2 and M1 sites (*Wood* and *Banno*, 1973). This assumption is made despite the unequal size of the two atoms; the fact that the M2 site in orthopyroxene is larger than the M1 site; or the fact that experimental evidence for this partitioning shows a distinct ordering between Fe^{2+} and Mg on the M1 and M2 sites (cf. *Anovitz* et al., 1988). Initially, for purposes of comparison, the ideal Fe^{2+}-Mg orthopyroxene mixing model of *Wood* and *Banno* (1973) is adopted. In this model, minor elements such as Ca and Mn are essentially treated as dilutents on the M2 site whereas Fe^{3+} and the remaining Al, not considered to substitute for Si, are treated as dilutents on the M1 site.

In contrast a variety of ternary (Fe,Mg,Ca) and quaternary (Fe,Mg,Ca,Mn) mixing models for garnet have been calibrated as new experimental data for various joins between endmember components in garnet have become available (e.g. *Ganguly* and *Kennedy*, 1974; *Perkins*, 1979; *O'Neill* and *Wood*, 1979; *Hodges* and *Spear*, 1982; *Newton* and *Perkins*, 1982; *Ganguly* and *Saxena*, 1984; *Sen* and *Bhattacharya*, 1984; *Newton* et al., 1986; *Wood*, 1987; *Berman*, 1990; *Lal*, 1993; *Berman* and *Aranovich*, 1996). Mixing along the Fe^{2+}-Mg join in these models has been suggested to range from ideal to relatively non-ideal, depending on the experimental data chosen for reference.

In this study, the *Berman* (1990) quaternary garnet mixing model is chosen due to its self consistency with the *Berman* (1988, 1990) data base; the fact that it incorporates the mixing properties of Mn as well as Fe^{2+}, Mg, and Ca in garnet; and the fact that it incorporates the most recent garnet mixing data available, e.g. *Koziol* and *Newton* (1989) and *Koziol* (1990), which allows it to build on earlier garnet mixing models. In constructing this mixing model, *Berman* (1990) uses the general excess equations derived by *Berman* and *Brown* (1985) with ternary excess mixing defined using the formulation contained in *Wohl* (1946, 1953). The mixing properties for a mineral component in the form of Margules parameters are then determined by pressure differences between end-member equilibria in P-T space and position of the same equilibria for a series of solid solutions. Excess volume of mixing data is also included which gives the individual component activities a pressure dependence. Mixing on the almandine-pyrope join is estimated to be relatively ideal. This is because the Fe^{2+}-Mg mixing parameters in this garnet mixing model are based on experimental Fe^{2+}-Mg K_D exchange data between almandine and orthopyroxene at relatively high pressures and temperatures ($P > 20$ kbars; $T > 900\,^{\circ}C$) (cf. *Kawasaki* and *Matsui*, 1983; *Harley*, 1984; *Lee* and *Ganguly*, 1988). At such high pressures and high temperatures, Fe^{2+}-Mg mixing in orthopyroxene, with some justification, is assumed to be relatively close to ideality. The Fe^{2+}-Mg K_D exchange data between garnet and orthopyroxene then forces mixing on the Fe^{2+}-Mg join in garnet to be relatively ideal as well. Near ideal mixing of Fe^{2+} and Mg in orthopyroxene at such high temperatures and pressures does not, of course, presume that they should mix ideally at granulite pressures and temperatures of 8 kbars and 800 °C though this is what is generally assumed. If anything, the converse should be true, i.e. mixing between Fe^{2+} and Mg in both garnet and orthopyroxene should be more non-ideal. Lastly, the ternary mixing parameter, C_{ijk}, for this mixing model is calculated to be close to 0 (cf. *Berman* and *Kozial*, 1991).

The mixing model for plagioclase is taken from *Newton* (1983) and derived from enthalpy of solution measurements on synthetic high structural state plagioclase by *Newton* et al. (1980) with the mixing entropy based on the "Al-avoidance" model. The free energy of mixing for this model agrees well with the free energy of mixing for plagioclase found by *Orville* (1972) in aqueous cation-exchange experiments at 700 °C.

Discussion

Pressures and temperatures were calculated iteratively using a series of FORTRAN computer programs with convergence usually after 3 to 4 iterations (*Peterson*, 1988). Temperatures and pressures are given in the first column in Table 4. Since the ΔV for Equilibrium (1) is relatively small, i.e. 0.098 J/bar, the difference in temperature calculated using the pressure estimated from either barometer is well within analytical error, i.e. $+/-10\,^{\circ}C$. Therefore in Table 4, to save space, a mean temperature is given along with the two pressures. The overall mean temperature is $800+/-60\,^{\circ}C$ (1σ). Mean pressures for the Alm-Fs and Pyr-En barometers are $9.2+/-1.0$ (1σ) kbar and $7.5+/-1.2$ (1σ) kbar respectively: a discrepancy of 1.7 kilobars. Plotting the difference in pressure between these two barometers, i.e.

Table 4. *Alm-Fs and Pyr-En pressures and temperatures*

	Ideal Fe-Mg Mixing in Gt and Opx				Non-Ideal Fe-Mg Mixing in Gt and Opx			
Sample	T (°C)	Alm-Fs P (kb)	Pyr-En P (kb)	ΔP (kb)	T (°C)	Alm-Fs P (kb)	Pyr-En P (kb)	ΔP (kb)
BD-17	742	9.64	8.02	1.63	735	7.64	7.63	0.01
BD-26	703	7.95	6.24	1.71	697	5.93	6.04	−0.11
BD-50	751	7.91	5.97	1.94	746	6.15	5.81	0.33
BD-58	764	8.06	5.87	2.19	760	6.60	5.66	0.94
BD-59	832	9.17	7.06	2.11	827	7.64	6.65	0.99
BD-60	829	9.23	6.99	2.25	823	7.57	6.49	1.08
BD-68	769	8.81	7.37	1.44	763	6.80	7.29	−0.48
BD-73	803	8.88	7.34	1.54	795	6.48	6.93	−0.46
BD-74	868	9.42	8.03	1.39	859	7.01	7.51	−0.51
BD-79	795	9.26	7.69	1.57	785	6.65	7.11	−0.46
BD-81	815	9.25	6.85	2.40	809	7.80	6.26	1.55
BD-83	825	9.09	6.86	2.23	820	7.58	6.50	1.08
BD-95	826	9.54	7.78	1.76	818	7.60	7.20	0.40
BD-102	721	8.00	6.44	1.56	715	6.18	6.33	−0.15
BD-136	879	10.07	8.28	1.79	872	7.89	7.85	0.03
BD-140	860	9.84	8.53	1.32	851	7.52	8.02	−0.50
BD-141	830	9.55	8.16	1.39	821	7.07	7.61	−0.54
BD-142	778	9.08	7.35	1.73	767	6.10	6.51	−0.41
BD-143	777	9.01	6.95	2.05	771	6.99	6.62	0.37
BD-301	831	9.51	7.13	2.38	824	8.47	5.69	2.78
BD-305	911	11.34	9.99	1.35	897	8.24	8.87	−0.62
BD-307	946	11.35	10.20	1.15	933	8.61	9.28	−0.67
BD-310	726	8.56	6.89	1.67	719	6.52	6.52	0.00
BD-312	700	7.18	5.41	1.77	697	5.74	5.47	0.27
BD-321	844	9.90	8.50	1.40	835	7.42	7.97	−0.55
BD-323	832	11.16	9.74	1.42	822	8.52	9.07	−0.55
BD-324	759	7.90	6.28	1.62	751	5.61	5.84	−0.23
BC-174	795	8.55	6.53	2.02	790	7.04	6.29	0.76
BC-276	799	9.84	7.40	2.44	791	7.89	6.45	1.44
BC-298	835	11.47	10.03	1.43	823	8.63	9.19	−0.56
BC-325	808	9.13	7.67	1.46	801	7.10	7.41	−0.32
AR-8	717	7.86	6.25	1.62	711	5.84	6.01	−0.17
AR-10	692	8.66	6.91	1.75	684	6.15	6.48	−0.32
AR-11	853	10.29	8.73	1.55	839	7.16	7.71	−0.56
AR-19	740	7.68	5.30	2.38	736	6.24	5.08	1.16
TV-6	866	9.76	7.75	2.01	859	7.87	7.31	0.56

$\Delta P = P_{Alm\text{-}Fs} - P_{Pyr\text{-}En}$, versus the total Fe fraction in orthopyroxene (X_{Fe}^{Opx}) (Fig. 2) where $X_{Fe}^{Opx} = (Fe^{2+}+Fe^{3+}) / 2.0$, results in a slightly linear positively sloped line totally above the $\Delta P = 0$ line. Similar plots are seen when ΔP is plotted against X_{Fe}^{Gt}, X_{Mg}^{Gt}, X_{Ca}^{Gt}, X_{Mn}^{Gt}, and X_{Ca}^{Plg}.

The source of the discrepancy seen in Fig. 2 has two possible origins. The first could be some sort of inconstancy in the standard enthalpies of reaction for

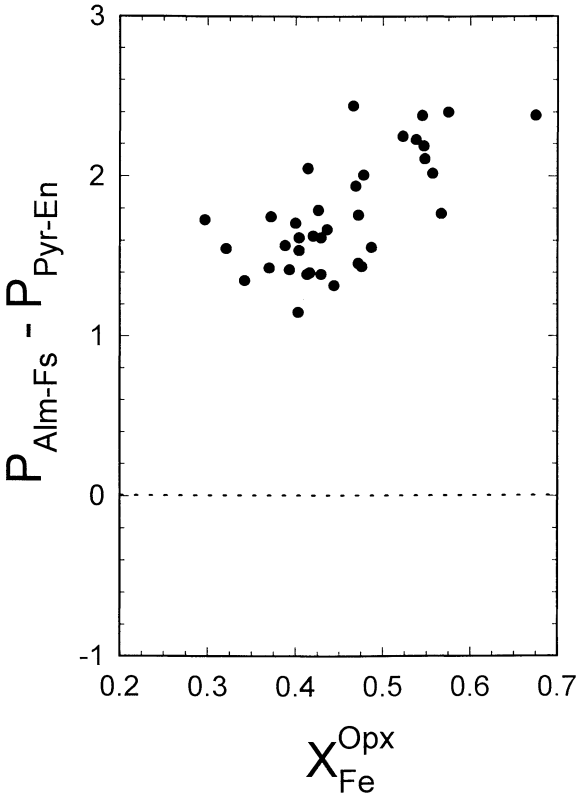

Fig. 2. Plot of relative pressure $\Delta P = P_{Alm\text{-}Fs} - P_{Pyr\text{-}En}$ vs. X_{Fe}^{Opx}. X_{Fe}^{Opx} is calculated as the total Fe fraction in orthopyroxene, i.e. $(Fe^{2+} + Fe^{3+})/2.0$. The garnet mixing model of *Berman* (1990) and the orthopyroxene mixing model of *Wood* and *Banno* (1973) are used. Mixing in plagioclase is calculated using *Newton* (1983)

Equilibria (2) and (3). However, this is highly unlikely considering the internal consistency of the *Berman* (1988, 1990) data base. More likely the origin for this discrepancy is due to the garnet, orthopyroxene, or plagioclase mixing models used. In this context, it is unlikely that the plagioclase mixing model is the source of the discrepancy. For example, if the mixing model of *Elkins* and *Grove* (1990) is utilized instead of *Newton* (1983), the pattern in ΔP vs X_{Fe}^{Opx} is remarkably similar to that seen in Fig. 2. This would suggest that the source of this discrepancy originates in the orthopyroxene and garnet mixing models used and not the plagioclase mixing model.

Experimental evidence suggests that mixing between Fe^{2+} and Mg in orthopyroxene is non-ideal with a positive departure from ideality. For example, Mossbauer resonance spectroscopy of quickly quenched, heat-treated natural and artificial orthopyroxenes indicates that Fe^{2+} and Mg are strongly partitioned between the M2 and M1 sites with Fe^{2+} being found preferentially on the larger M2 site and Mg on the smaller M1 site (*Anovitz* et al., 1988; *Ganguly*, 1982; *Besancon*, 1981; *Saxena*, 1973; *Saxena* and *Ghose*, 1971; *Virgo* and *Hafner*, 1970). This partitioning is more prominent at lower temperatures (500–900 °C) and less prominent at higher temperatures (>1000 °C). The pronounced ordering of Fe^{2+} and Mg on the M1 and M2 sites implies a large negative deviation in the entropy of disorder and consequently a positive enthalpy of mixing at granulite facies pressures and temperatures (5–10 kb, 600–900 °C) which has been confirmed, in part, by *Chatillon-Colinet* et al. (1983). Other experimental evidence includes the reversed EMF experiments on a range of ferrosilite-enstatite solid solutions at

1000 K by *Sharma* et al. (1987) which indicate a large positive departure from ideality for Fe^{2+}-Mg mixing in orthopyroxene. In addition, experimental data contained in *Kawasaki* and *Matsui* (1983) in the form of unequal Fe^{2+}-Mg partitioning data between orthopyroxene-garnet, orthopyroxene-olivine and garnet-olivine suggests that Fe^{2+}-Mg mixing in orthopyroxene is non-ideal.

In response we adopt the non-ideal symmetric regular Fe^{2+}-Mg orthopyroxene mixing model of *Sack* and *Ghiorso* (1989) which exhibits a positive departure from ideality. This model is chosen, in part, due to its internal consistency with most experimental data on Fe^{2+}-Mg mixing in orthopyroxene listed above as well as its self consistency with the *Berman* (1988, 1990) data base. It makes provision for the non-convergent ordering of Fe^{2+} and Mg between the M1 and M2 sites in orthopyroxene, non-idealities in the substitutions of Fe^{2+} and Mg on these sites, and non-zero enthalpies of reciprocal ordering of Fe^{2+} and Mg between the two sites. In addition, this mixing model is consistent with constraints provided by experimental and natural data on the Fe^{2+} and Mg exchange reaction between olivine and orthopyroxene +/− quartz, Mossbauer M2 and M1 site occupancy data on orthopyroxenes, enthalpy of solution and disordering data on orthopyroxenes, available data on the temperature and ordering dependence of the excess volume of orthopyroxene solid solutions, and direct activity-composition determinations of orthopyroxene solid solutions at elevated temperatures. However this mixing model does not take into account the effect of minor cations such as Al, Fe^{3+}, Ca, and Mn with respect to mixing on the Fe^{2+}-Mg join. The principal minor cation in the orthopyroxene from the Bamble samples is Al of which the majority is assumed to substitute for Si on the tetrahedral site (Tables 2 and 3). Since X_{Fe}^{Opx} and X_{Mg}^{Opx} used in the activity calculations are determined as the ratio of Fe^{2+} or Mg over the sum (Fe^{3+}+Fe^{2+}+Mg), Mn, Ca, and "left over" Al, assumed not on the tetrahedral site, are essentially treated as a dilutent.

If this orthopyroxene mixing model is adopted, then mixing on the Fe^{2+}-Mg join in garnet must be adjusted using the Fe^{2+}-Mg exchange data between garnet and orthopyroxene (e.g. *Lee* and *Ganguly*, 1988) to reflect this non-ideality in orthopyroxene such that mixing along the Fe^{2+}-Mg join in both garnet and orthopyroxene is now internally self consistent and exhibit the same moderate positive departure from ideality. In concordance with their orthopyroxene mixing model, *Sack* and *Ghiorso* (1989) have calibrated a set of symmetric Margules mixing parameters ($W_{FeMg}^{H} = W_{MgFe}^{H} = 16110$ J/gfw) for the Fe^{2+}-Mg join in garnet which results in a moderate, non-temperature dependent, positive departure from ideality. In this calibration they assume that W_{FeMg}^{G} and W_{MgFe}^{G}, where $W^G = W^H - TW^S + PW^V$, have a negligible dependence temperature dependence, i.e. $W^S = 0$.

Plugging these values for W_{FeMg}^{G} and W_{MgFe}^{G} into the *Berman* (1990) garnet mixing model while allowing for the same pressure dependence, i.e. using Berman's values for W^V along the Fe^{2+}-Mg join (cf. *Berman*, 1990), results in Fig. 3 and the second series of columns in Table 4. The data now straddles the $\Delta P = 0$ line and the pressures are mostly within +/−1 kilobar of each other per sample. The mean values for $P_{Alm\text{-}Fs}$ and $P_{Pyr\text{-}En}$ are now 7.1+/−0.9 (1σ) and 7.0+/−1.1 (1σ) kbars respectively with the mean temperature at 793+/−58 °C (1σ). With the exception of one point at $X_{Fe}^{Opx} = 0.675$, the two barometers are obviously in much better agreement. If maintaining internal consistency between the orthopyroxene and

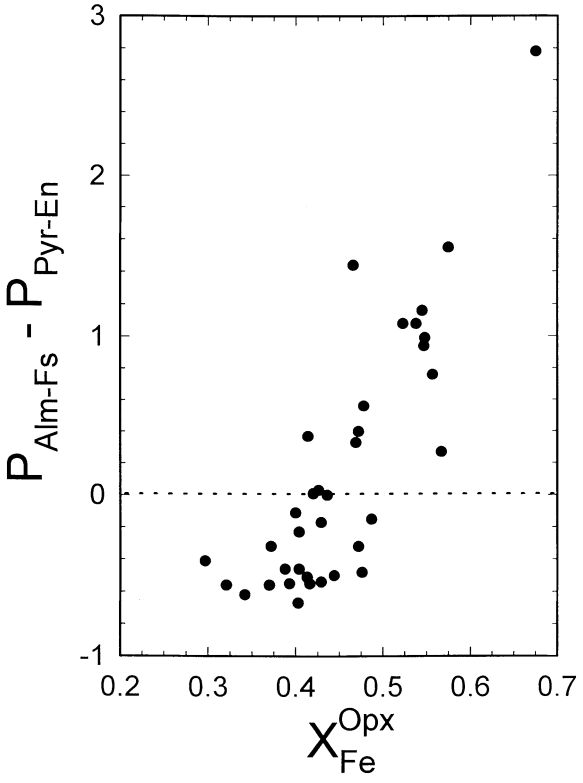

Fig. 3. Plot of relative pressure $\Delta P = P_{Alm\text{-}Fs} - P_{Pyr\text{-}En}$ vs. X_{Fe}^{Opx}. X_{Fe}^{Opx} is calculated as the total Fe fraction in orthopyroxene, i.e. $(Fe^{2+} + Fe^{3+})/2.0$. The garnet mixing model of *Berman* (1990), adjusted such that now $W_{FeMg}^{H} = W_{MgFe}^{H} = 16110$ J/mole, and the orthopyroxene mixing model of *Sack* and *Ghiorso* (1989) are used. Mixing in plagioclase is calculated using *Newton* (1983)

garnet mixing models is neglected such that the original *Berman* (1990) garnet mixing model (ideal Fe^{2+}-Mg mixing) is used in conjunction with the *Sack* and *Ghiorso* (1989) orthopyroxene mixing model (non-ideal Fe^{2+}-Mg mixing), the discrepancy between the two barometers seen in Fig. 2 actually increases.

The mean temperature (792 °C) and pressures (7.1 and 7.0 kb) from Table 4 and Fig. 3 fall well within the stability range of sillimanite and are also in reasonable agreement with a temperature and pressure of 800 °C and 8 kb obtained by *Touret* (1971) from CO_2 fluid inclusion data. Good agreement with these pressures is also seen in the presence of Mg rich cordierite ($X_{Mg}^{Cd} = 0.82$) which places an upper limit of 7.6 kilobars on the pressure at 792 °C (*Holdaway* and *Lee*, 1977; *Newton* and *Wood*, 1979). A mean temperature of 792 °C is also in excellent agreement with a similar mean temperature of 795 °C +/−60 °C (1σ) obtained from non-reset titaniferous magnetite-ilmenite grains (*Harlov*, 1992) using the titaniferous magnetite-ilmenite thermometer of *Ghiorso* and *Sack* (1991) on some of the samples used in this study as well as others from Region D. The resulting temperature distribution in Region D calculated using these non-ideal garnet and orthopyroxene mixing models and tabulated in Table 4 is shown in Fig. 4.

Remaining discrepancies between $P_{Alm\text{-}Fs}$ and $P_{Pyr\text{-}En}$ in Fig. 3 are most likely due to the fact that the effect of minor cations such as Ca, Mn and Al is not taken into account in the Fe^{2+}-Mg orthopyroxene mixing model of *Sack* and *Ghiroso* (1989). This can especially be seen when ΔP is graphed against X_{Ca}^{Opx}, X_{Mn}^{Opx} and X_{Al}^{Opx} in Figs. 5a–5c. What is especially striking is the strong correlation when ΔP

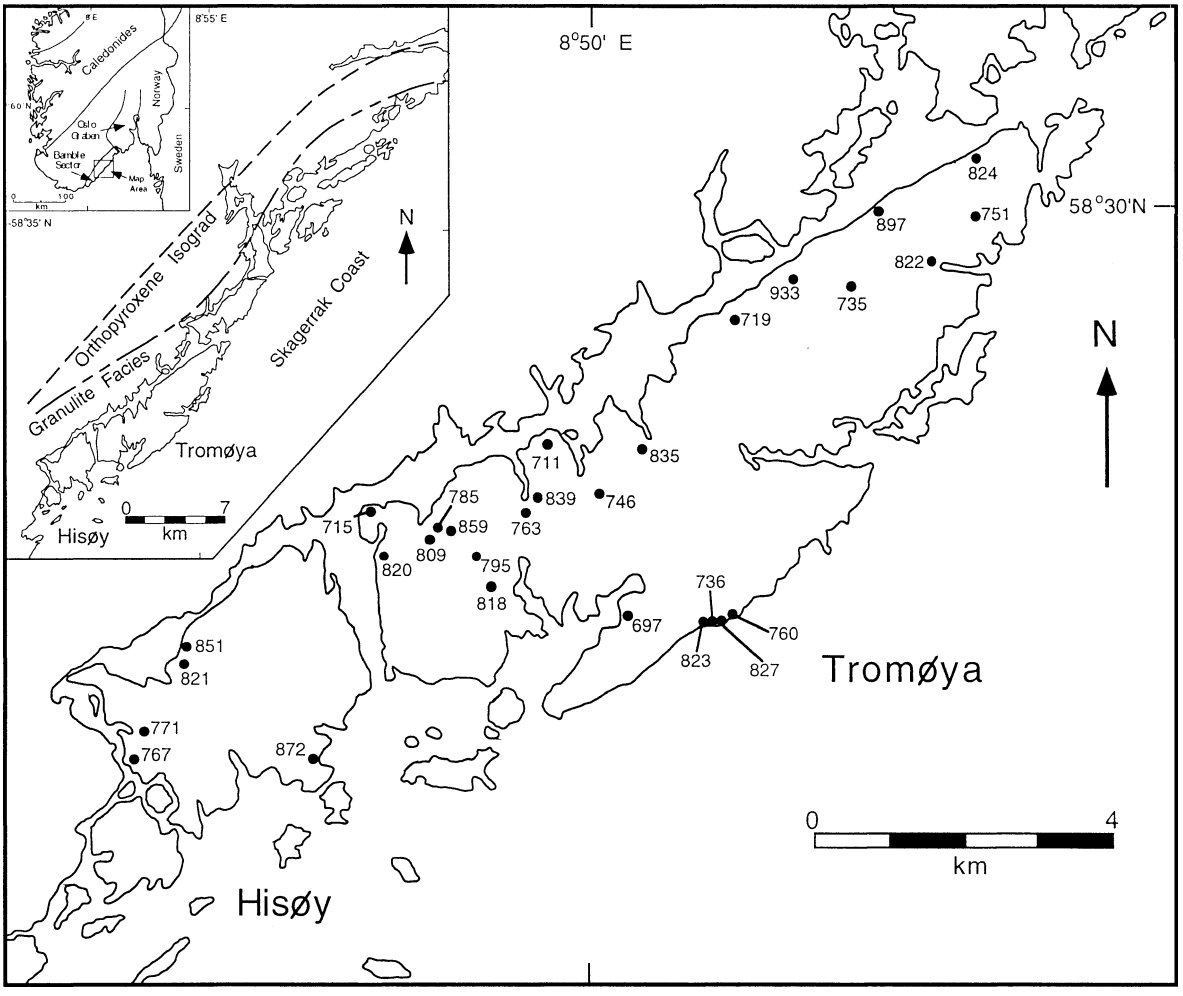

Fig. 4. Distribution of garnet-orthopyroxene K_D exchange temperatures in Region D of the Bamble Sector, i.e. the islands of Tromøya and Hisøya. Temperatures are taken from Table 4 for the case when the garnet mixing model of *Berman* (1990), adjusted such that now $W^H_{\mathrm{FeMg}} = W^H_{\mathrm{MgFe}} = 16110$ J/mole, and the orthopyroxene mixing model of *Sack* and *Ghiorso* (1989) are used. Temperatures from samples 86-BC-174, 86-BC-276, 86-BC-298, 86-BC-325, and 84-TV-6 are not plotted since the locations of these samples are in Region C. Two additional samples, 86-BD-26 and 84-AR-8, and are also not plotted since they are located at the same locations as two other samples in Table 2

is graphed vs. $X^{\mathrm{opx}}_{\mathrm{ca}}$ (cf. Fig. 5a). This would seem to suggest that even minor amounts of Ca in orthopyroxene have a strong influence on the calibration of this orthopyroxene Fe^{2+}-Mg mixing model. Plots of ΔP vs. $X^{\mathrm{Opx}}_{\mathrm{Mn}}$ and $X^{\mathrm{Opx}}_{\mathrm{Al}}$ (cf. Figs. 5b and 5c) are less dramatic but still show a relatively linear trend suggesting that mixing by these cations also plays some role in influencing mixing between Fe^{2+} and Mg in orthopyroxene. In distinct contrast, plots of $X^{\mathrm{Gt}}_{\mathrm{Fe}}, X^{\mathrm{Gt}}_{\mathrm{Mg}}, X^{\mathrm{Gt}}_{\mathrm{Ca}}$ or $X^{\mathrm{Gt}}_{\mathrm{Mn}}$ vs ΔP show no such distinct correlation's suggesting, again, that the garnet mixing parameters involved are least somewhat correctly compensating for the mixing properties of these cations in garnet. Likewise, if the plagioclase mixing model of

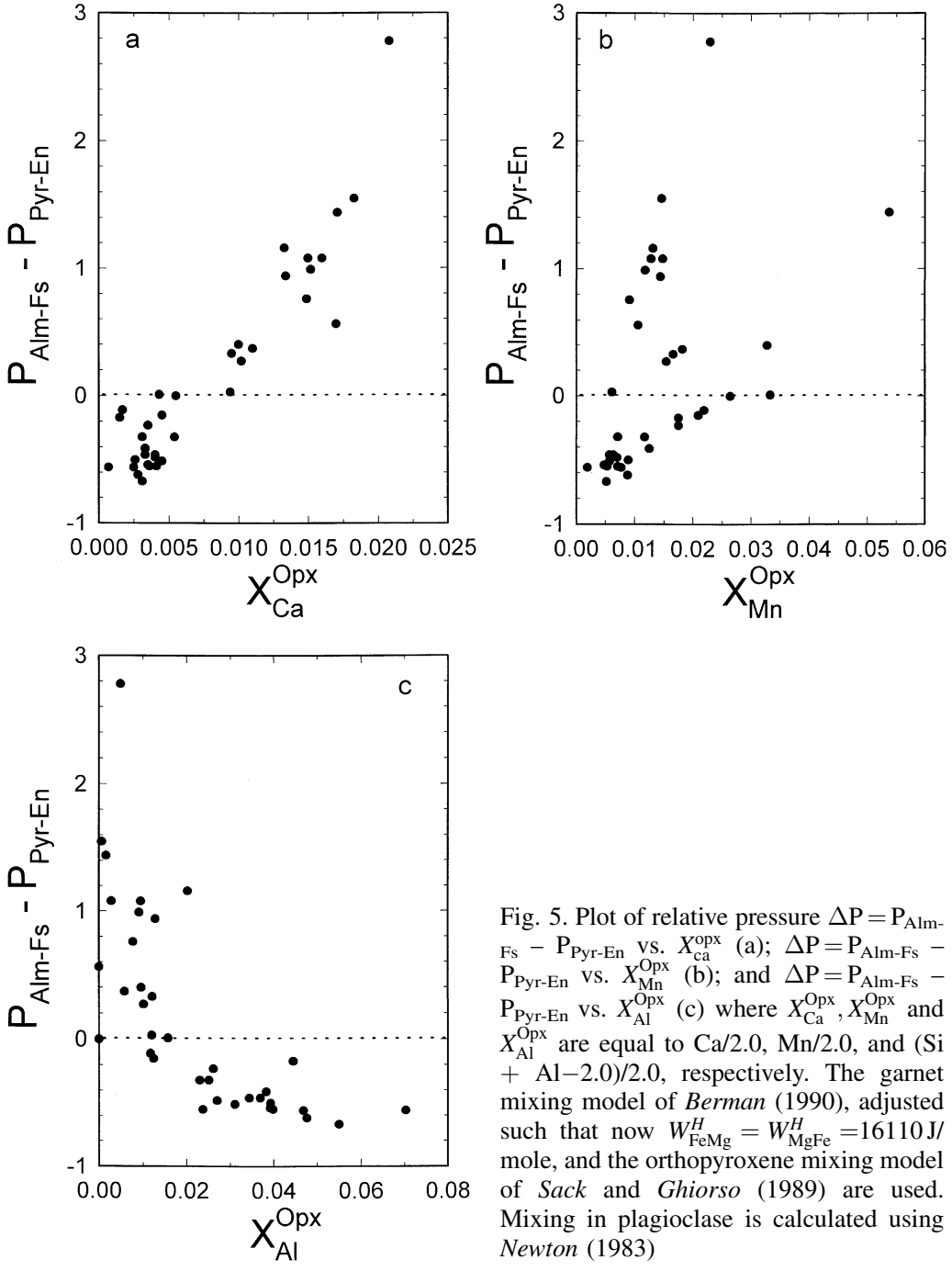

Fig. 5. Plot of relative pressure $\Delta P = P_{Alm-Fs} - P_{Pyr-En}$ vs. X^{opx}_{ca} (a); $\Delta P = P_{Alm-Fs} - P_{Pyr-En}$ vs. X^{Opx}_{Mn} (b); and $\Delta P = P_{Alm-Fs} - P_{Pyr-En}$ vs. X^{Opx}_{Al} (c) where $X^{Opx}_{Ca}, X^{Opx}_{Mn}$ and X^{Opx}_{Al} are equal to Ca/2.0, Mn/2.0, and (Si + Al−2.0)/2.0, respectively. The garnet mixing model of *Berman* (1990), adjusted such that now $W^H_{FeMg} = W^H_{MgFe}$ =16110 J/mole, and the orthopyroxene mixing model of *Sack* and *Ghiorso* (1989) are used. Mixing in plagioclase is calculated using *Newton* (1983)

Elkins and *Grove* (1990) is utilized along with the *Sack* and *Ghiorso* (1989) orthopyroxene mixing model and the adjusted *Berman* (1990) garnet mixing model, little change is seen. Pressures for the Alm-Fs and Pyr-En barometers average 7.0+/−0.6 (1σ) and 6.8+/−0.8 (1σ) respectively and a pattern in ΔP vs X^{Opx}_{Fe}, identical to that seen in Fig. 3, occurs. It is interesting to note that plotting

ΔP vs. X_{Ca}^{Opx}, X_{Mn}^{Opx} or X_{Al}^{Opx}, when the ideal orthopyroxene mixing model of *Wood* and *Banno* (1973) is used, does not produce the dramatic contrasts seen in Figs. 5a–5c. This is perhaps due to the fact that in this mixing model, Ca, Mn and Al are assigned to either the M1 or the M2 sites and as a consequence their effect on Fe^{2+}-Mg mixing is somewhat crudely compensated for.

Conclusions

The results of this study emphasize the importance of selecting garnet and orthopyroxene mixing models which are internally self consistent via experimental K_D exchange data as well as the thermochemical data base used for stoichiometric endmember components. They suggest that Fe^{2+}-Mg mixing in orthopyroxene and garnet is probably non-ideal at granulite facies pressures and temperatures. The existence of a positive slope seen when ΔP is graphed vs X_{Fe}^{Opx}, X_{Ca}^{Opx}, X_{Mn}^{Opx} or X_{Al}^{Opx} in Figs. 3 and 5 suggests that the effect of minor components in calibrating a orthopyroxene Fe^{2+}-Mg mixing model is probably important. Lastly this result is not affected by the application of different plagioclase mixing models.

Acknowledgments

I thank *J. Valley* for initially introducing me to the granulites of the Bamble region and the financial support he so generously provided, *R. Newton* for many useful discussions, *E. Glover* for his aid in the use of the microprobe and *P. Dombrawski* for help in drafting some of the figures. I also thank *C. Schmidt*, *D. Pattison*, *R. Berman*, *J. Ganguly, D. Perkins, J. B. H. Hansen* and *E. Essene* for very useful reviews of an earlier draft of this paper. I also thank *T. Gerya* for his comments on the present version of this paper. This work was supported by NSF Grants EAR-8508102 and EAR-8805470 (to *J. Valley*); Gas Research Institute Grants 5083-260-08521 and 5086-260-1425 (to *J. Valley*); Sigma Xi (to *D. Harlov*); and the Department of Geology and Geophysics, University of Wisconsin (to *D. Harlov*).

References

Anovitz LM, Essene EJ, Dunham WR (1988) Order-disorder experiments on orthopyroxene: implications for the orthopyroxene geospeedomenter. Am Mineral 73: 1060–1073

Bence AE, Albee AL (1968) Empirical correction factors for the electron microanalysis of silicates and oxides. J Geol 76: 382–403

Berman RG (1988) Internally-consistent thermodynamic data for minerals in the system Na_2O-K_2O-CaO-MgO-FeO-Fe_2O_3-Al_2O_3-SiO_2-TiO_2-H_2O-CO_2. J Petrol 29: 445–522

Berman RG (1990) Mixing properties of Ca-Mg-Fe-Mn garnets. Am Mineral 75: 328–344

Berman RG, Brown TH (1985) A thermodynamic model for multicomponent melts, with application to the system CaO-Al_2O_3-SiO_2. Geochim Cosmochim Acta 48: 661–678

Berman RG, Koziol AM (1991) Ternary excess properties of grossular-pyrope-almandine garnet and their influence on geothermobarometry. Am Mineral 76: 1223–1231

Berman RG, Aranovich L Ya (1996) Optimized standard state and solution properties of minerals I. Model calibration for olivine, orthopyroxene, cordierite, garnet, and ilmenite in the system FeO-MgO-CaO-Al_2O_3-TiO_2-SiO_2. Contrib Mineral Petrol 126: 1–24

Besancon JR (1981) Rate of cation ordering in orthopyroxenes. Am Mineral 66: 965–973

Bohlen SR, Essene EJ, Boettcher AL (1980) The investigation and application of olivine-quartz-orthopyroxene barometry. Earth Planet Sci Lett 47: 1–10

Bohlen SR, Wall VJ, Boettcher AL (1983) Experimental investigation and application of garnet granulite equilibria. Contrib Mineral Petrol 83: 52–61

Cameron EM, Cogulu EH, Stirling J (1993) Mobilization of gold in the deep crust: evidence from mafic intrusions in the Bamble belt, Norway. Lithos 30: 151–166

Chatillon-Colinet C, Kleppa OJ, Newton RC, Perkins D (1983) Enthalpy of formation of $Fe_3Al_2Si_3O_{12}$ (almandine) by high temperature alkali borate solution calorimetry. Geochim Cosmochim Acta 47: 439–444

Eckert JO, Bohlen SR (1992) Reversed experimental determinations in the Mg-Fe^{2+} exchange equilibrium in Fe-rich garnet-orthopyroxene pairs. Transact Am Geophys Union (EOS) 73: 608

Elkins LT, Grove TL (1990) Ternary feldspar experiments and thermodynamic models. Am Mineral 75: 544–559

Field D, Drury SA, Cooper DC (1980) Rare-earth and LIL element fractionation in high-grade charnockitic gneisses, South Norway. Lithos 13: 281–289

Field D, Smalley PC, Lamb RC, Raheim A (1985) Geochemical evolution of the 1.6-1.5 Ga old amphibolite-granulite facies terrain, Bamble Sector, Norway: dispelling the myth of grenvillian high-grade reworking. In: *Tobi AC*, *Touret JLR* (eds) The Proterozoic crust in the North Atlantic Provinces. Reidel, Berlin, pp 567—578

Ganguly J (1982) Mg-Fe order-disorder in ferromagnesian silicates II. Thermodynamics, kinetics, and geological applications. In: *Saxena SK* (ed) Advances in physical geochemistry. Springer, Berlin Heidelberg New York Tokyo, pp 58–99

Ganguly J, Kennedy GC (1974) The energetics of natural garnet solid solution. I. Mixing of the aluminosilicate end-members. Contrib Mineral Petrol 48: 137–148

Ganguly J, Saxena SK (1984) Mixing properties of aluminosilicate: constraints from natural and experimental data, and applications to geo-thermo-barometry. Am Mineral 69: 88–97

Ghiorso MS, Sack RO (1991) Fe-Ti oxide geothermometry: thermodynamic formulation and the estimation of intensive variables in silicic magmas. Contrib Mineral Petrol 108: 485–510

Haglia P (1995) Rb-Sr-systematics of the Proterozoic Bamble and Telemark sectors, south Norway: myths and reality. Geonytt 22: 33–34

Harley SL (1984) An experimental study of the partitioning of Fe and Mg between garnet and orthopyroxene. Contrib Mineral Petrol 86: 359–373

Harlov DE (1992) Comparative oxygen barometry in granulites, Bamble Sector, S.E. Norway. J Geol 100: 447–464

Harlov DE, Hansen EC, Bigler C (1998) Petrologic evidence for K-feldspar metasomatism in granulite facies rocks. Chem Geol 151: 373–386

Hodges KV, Spear FS (1982) Geothermometry, geobarometry and the Al_2SiO_5 triple point at Mt. Moosilauke, New Hampshire. Am Mineral 67: 1118–1134

Holdaway MJ, Lee SM (1977) Fe-Mg cordierite stability in high-grade pelitic rocks based on experimental, theoretical, and natural observations. Contrib Mineral Petrol 63: 175–198

Holland TJB, Powell R (1990) An enlarged internally consistent thermodynamic data set with uncertainties and correlation's: the system K_2O-Na_2O-CaO-MgO-MnO-FeO-Fe_2O_3-Al_2O_3-TiO_2-SiO_2-C-H_2-O_2. J Met Geol 8: 89–124

Kawasaki T, Matsui Y (1983) Thermodynamic analyses of equilibria involving olivine, orthopyroxene, and garnet. Geochim Cosmochim Acta 47: 1661–1679

Koziol AM (1990) Activity-composition relationships of binary Ca-Fe and Ca-Mn garnets determined by reversed, displaced equilibrium experiments. Am Mineral 75: 319–327

Koziol AM, Newton RC (1989) Grossular activity-composition relationships in ternary garnet determined by reversed displaced-equilibrium experiments. Contrib Mineral Petrol 103: 423–433

Kullerud L, Dahlgren S (1993) Sm-Nd geochronology of Sveconorwegian granulite facies mineral assemblages in the Bamble shear belt, South Norway. Prec Res 64: 389–402

Lal RK (1993) Internally consistent recalibrations of mineral equilibria for geothermobarometry involving garnet-orthopyroxene-plagioclase-quartz assemblages and their application to the South Indian granulites. J Met Geol 11: 855–866

Lamb RC, Smalley PC, Field D (1986) P-T conditions for the Arendal Granulites, Southern S.E. Norway: implications for the roles of P, T, and CO_2 in deep crustal LILE – depletion. J Met Geol 4: 143–160

Lee HY, Ganguly J (1988) Equilibrium compositions of co-existing garnet and orthopyroxene: reversed experimental determinations in the system FeO-MgO-Al_2O_3-SiO_2 and applications. J Petrol 29: 93–113

Moecher DP, Essene EJ, Anovitz LJ (1988) Calculation of clinopyroxene-garnet-plagioclase-quartz geobarometers: evaluation and application to high grade metamorphic rocks. Contrib Mineral Petrol 100: 92–106

Newton RC (1983) Geobarometry of high grade metamorphic rocks. Am J Sci 283-A: 1–28

Newton RC, Wood BJ (1979) Thermodynamics of water in cordierite and some petrologic consequences of cordierite as a hydrous phase. Contrib Mineral Petrol 68: 391–405

Newton RC, Perkins D (1982) Thermodynamic calibration of geobarometers based on the assemblages garnet-plagioclase-orthopyroxene-(clinopyroxene)-quartz. Am Mineral 67: 203–222

Newton RC, Charlu TV, Kleppa OJ (1980) Thermochemistry of the high structural state plagioclases. Geochim Cosmochim Acta 44: 933–941

Newton RC, Geiger CA, Kleppa OJ, Brouse C (1986) Thermochemistry of binary and ternary garnet solid solutions. IMA Abstr with Prog: 186

Orville PM (1972) Plagioclase cation exchange equilibria with aqueous chloride solution: results at 700 °C and 2000 bars in the presence of quartz. Am J Sci 272: 234–272

O'Neill H St C, Wood BJ (1979) An experimental study of Fe-Mg partitioning between garnet and olivine and its calibration as a geothermometer. Contrib Mineral Petrol 70: 59–70

Perkins D (1979) Application of new thermodynamic data to mineral equilibria. Thesis, University of Michigan, Ann Arbor (unpublished)

Perkins D, Chipera SJ (1985) Garnet-orthopyroxene-plagioclase-quartz barometry: refinement and application to the English River subprovince and the Minnesota River Valley. Contrib Mineral Petrol 89: 69–80

Peterson DE (1988) Application of geothermometry, geobarometry and oxygen barometry to the LIL/REE depleted granulite facies terrane in the Bamble Sector, Southeast Norway. Thesis, University of Wisconsin, Madison (unpublished)

Sack RO, Ghiorso MS (1989) Importance of considerations of mixing properties in establishing an internally consistent thermodynamic data base: thermochemistry of minerals in the system Mg_2SiO_4-Fe_2SiO_4-SiO_2. Contrib Mineral Petrol 102: 41–68

Saxena SK (1973) Thermodynamics of rock-forming crystalline solutions. Springer, Berlin Heidelberg New York Tokyo, pp 90–112

Saxena SK, Ghose S (1971) Mg^{2+}-Fe^{2+} order-disorder and the thermodynamics of orthopyroxene crystalline solution. Am Mineral 56: 532–559

Sen SK, Bhattacharya A (1984) An orthopyroxene-garnet thermometer and its application to the Madras charnockites. Contrib Mineral Petrol 88: 64–71

Sharma KC, Agrawal RD, Kapoor ML (1987) Determination of thermodynamic properties of (Fe,Mg)-pyroxenes at 1000 K by the EMF method. Earth Planet Sci Lett 85: 302–310

Smalley PC, Field D, Lamb RC, Clough PWL (1983) Rare earth, Th-Hf-Ta and large-ion lithophile element variations in metabasites from the proterozoic amphibolite-granulite transition zone at Arendal, South Norway. Earth Planet Sci Lett 63: 446–458

Starmer IC (1985) The evolution of the South Norwegian Proterozoic as revealed by the major and mega-tectonics of the Kongsberg and Bamble Sectors. In: *Tobi AC, Touret JLR* (eds) The Deep Proterozoic crust in the North Atlantic Provinces. Reidel, Berlin, pp 259–290

Starmer IC (1986) Geological Map of the Bamble Sector, South Norway (1:100,000): 3 Sheets. NATO Advanced Study Institute 1984 Excursion Guide. In: *Maijer C*, *Padget P* (eds) The geology of Southernmost Norway: an excursion guide. Norges Geologiske Undersokelse, Spec Publ 1 (1987): 109 pp

Touret JLR (1971) le Facies granulite en Norvege Meridional II: le inclusions fluides. Lithos 4: 423–436

Touret JLR (1985) Fluid regime in Southern Norway: the record of fluid inclusions. In: *Tobi AC, Touret JLR* (eds) The Deep Proterozoic crust in the North Atlantic Provinces. Reidel, Berlin, pp 517–549

Touret JLR, Falkum T (1984) The high grade metamorphic Bamble Sector. In: *Maijer C* (ed) Excursion Guide of the South Norway Geological Excursion: 27–42

Virgo D, Hafner SS (1970) Fe^{2+}, Mg order-disorder in natural orthopyroxenes. Am Mineral 55: 210–223

Visser D, Senior A (1990) Aluminous reaction textures in orthoamphibole-bearing rocks: the pressure-temperature evolution of the high-grade Proterozoic of the Bamble sector, South Norway. J Met Geol 8: 231–246

Wood BJ (1987) Thermodynamics of multicomponent systems containing several solid solutions. In: *Carmichael ISE, Eugster HP* (eds) Thermodynamic modeling of geological materials: minerals, fluids and melts. MSA Short Course 17: 71–95

Wood BJ, Banno S (1973) Garnet-orthopyroxene and orthopyroxene-clinopyroxene relationships in simple and complex systems. Contrib Mineral Petrol 42: 109–124

Wohl K (1946) Thermodynamic evaluation of binary and ternary liquid systems. Trans Am Inst Chem Eng 42: 215–249

Wohl K (1953) Thermodynamic evaluation of binary and ternary liquid systems. Chem Eng Prog 49: 218–219

Author's address: Dr. *D. E. Harlov*, GeoForschungsZentrum Potsdam, Telegrafenberg, D-14473 Potsdam, Federal Republic of Germany